

# Breaking the CCSD(T) Barrier for Machine Learned Potentials of Large Molecules: Demonstration for Acetylacetone

Chen Qu<sup>1</sup>, Paul Houston<sup>2</sup>, Riccardo Conte<sup>3</sup>, Apurba Nandi<sup>4</sup>, and Joel M. Bowman<sup>4,\*</sup>

<sup>1</sup>Department of Chemistry & Biochemistry, University of Maryland, College Park, Maryland 20742, U.S.A.

<sup>2</sup>Department of Chemistry and Chemical Biology, Cornell University, Ithaca, New York 14853, U.S.A. and Department of Chemistry and Biochemistry, Georgia Institute of Technology, Atlanta, Georgia 30332, U.S.A

<sup>3</sup>Dipartimento di Chimica, Università degli Studi di Milano, via Golgi 19, 20133 Milano, Italy

<sup>4</sup>Department of Chemistry and Cherry L. Emerson Center for Scientific Computation, Emory University, Atlanta, Georgia 30322, U.S.A.

\*Corresponding author: jmbowma@emory.edu

## ABSTRACT

Machine-learned potential energy surfaces (PESs) for molecules with more than 10 atoms are typically forced to use lower-level electronic structure methods such as density functional theory and second-order Møller-Plesset perturbation theory (MP2). While these are efficient and realistic, they fall short of the accuracy of the “gold standard” coupled-cluster method [CCSD(T)], especially with respect to reaction and isomerization barriers. We report a major step forward in using a  $\Delta$ -machine learning method to the challenging case of acetylacetone, whose MP2 barrier height for H-atom transfer is low by roughly 1.5 kcal/mol relative to the CCSD(T) barrier of 3.5 kcal/mol. From a database of 2151 LCCSD(T) energies, and training with as few as 430 energies, we obtain a new PES with a barrier in agreement with the LCCSD(T) one. Tunneling splittings due to H-atom transfer are calculated using this new PES, providing improved estimates over previous ones obtained using an MP2-based PES.

## Introduction

There has been dramatic progress in using regression methods from machine learning (ML) to develop potential energy surfaces (PESs) for systems with more than five atoms, based on fitting thousands of CCSD(T) energies.<sup>1–4</sup>

However, the CCSD(T) method, because it scales as  $N^7$  where  $N$  is the system size, is too computationally demanding for PES fits of systems with more than 10 heavy atoms. (This number of atoms is rightly not considered a “large molecule” by many readers; however, it is used here as a computational boundary for the CCSD(T) method.) One 10-atom we are aware of is the formic acid dimer ( $\text{HCOOH}$ )<sub>2</sub>,<sup>5</sup> which contains 8 heavy atoms. This was a major computational effort at the CCSD(T)-F12a/haTZ (VTZ for H and aVTZ for C and O) level of theory. This PES, which does not dissociate, was obtained with only 13 475 energies. A 9-atom PES for the chemical reaction  $\text{Cl}+\text{C}_2\text{H}_6$  system was recently reported using a composite MP2/CCSD(T) method.<sup>6</sup> Both of these PESs were fit using Permutationally Invariant Polynomial (PIP) regression. Examples of potentials for 6 and 7-atom chemical reactions which are fits to tens or even hundred thousand CCSD(T) energies have also been reported.<sup>1,3,4,7,8</sup>

The 10-atom CCSD(T)-barrier is due both to the steep scaling with  $N$  and the increasing dimensionality of the PES, which requires larger data sets. Thus, given the intense interest, and progress, in moving to larger molecules and clusters, where high-level methods are prohibitively expensive, the use of lower-level

methods such as Density Functional Theory (DFT) and second-order Møller-Plesset perturbation (MP2) theory, is understandable. These methods also provide analytical gradients and this is an important source of data needed for larger systems. Our group has made use of this approach for PIP PESs of *N*-methyl acetamide,<sup>9,10</sup> glycine<sup>11</sup> and tropolone.<sup>12</sup>

We recently reported PIP and fragmented PIP PESs (see below for some details) for 15-atom acetylacetone (AcAc),<sup>13</sup> using MP2 energies and gradients from Meuwly and co-workers,<sup>14</sup> supplemented by roughly 500 additional configurations. The former PES (which is exploited here) produces a barrier for symmetric H-atom transfer of 2.13 kcal/mol ( $745\text{ cm}^{-1}$ ) in close agreement with the direct MP2 value of 2.18 kcal/mol ( $763\text{ cm}^{-1}$ ). However, that value of the barrier is more than 1 kcal/mol below the reported CCSD(T)/aug-cc-pVTZ one of 3.2 kcal/mol.<sup>15</sup> It is expected that this error in the MP2-based PES leads to a large overestimate of the tunneling splitting for the ground vibrational state H-atom transfer. Nevertheless, the splitting was obtained with the MP2-based PES, using full-dimensional diffusion Monte Carlo calculations. The splitting is  $160\text{ cm}^{-1}$  with an uncertainty of  $15\text{ cm}^{-1}$ . Using a simple 1d model, a splitting of  $113\text{ cm}^{-1}$  was obtained for a barrier of 2.2 kcal/mol and  $74\text{ cm}^{-1}$  for scaled barrier of 3.2 kcal/mol. This simple 1d estimate for the larger barrier is not expected to be quantitative; however, it does confirm that a large decrease in the splitting with increasing the barrier by 1 kcal/mol can be expected.

This magnitude of the error in chemical barriers is typical for MP2 and DFT accuracy, compared to benchmark CCSD(T) results. In addition, harmonic frequencies of XH-stretch modes are typically underestimated by of the order of  $100\text{ cm}^{-1}$  using popular DFT approaches. Thus, there is a strong motivation to improve a PES based on a lower-level method such as DFT and MP2.

Recent approaches to this, using ML, aim to bring a PES based on a low-level of electronic theory to a higher level. There are two approaches currently being investigated to accomplish this goal. One is transfer learning, which has been developed extensively in the context of artificial neural networks,<sup>16</sup> and much of the work in that field has been brought into chemistry.<sup>14,17-20</sup> The basic idea of transfer learning is that a fit obtained from one source of data (perhaps a large one) can be corrected by using limited data and by making hopefully small training alterations to the parameters obtained in the first fit. So, in the present context of PES fitting, a ML-PES fit to low-level electronic energies/gradients can be reused as the starting point of the model for a different task, e.g., an ML-PES with the accuracy of a high-level electronic structure theory. As noted, this is typically done with artificial neural works, where weights and biases trained on lower-level data hopefully require minor changes in response to additional training using high-level data.

The other approach is “ $\Delta$ -machine learning”. In this approach a correction is made to a property obtained using an efficient, low-level *ab initio* theory.<sup>14,18-21</sup> The focus of most work on transfer learning or  $\Delta$ -learning has been on developing transferable force fields, with applications mainly in the thermochemistry and molecular dynamics simulations.

Meuwly and co-workers applied transfer learning using thousands of local CCSD(T) energies to improve their MP2-based neural network PESs for malonaldehyde, acetoacetaldehyde and acetylacetone.<sup>14</sup> We recently proposed and tested a  $\Delta$ -learning approach, which uses a small number of CCSD(T) energies, to correct a PES based on DFT electronic energies and gradients.<sup>22</sup> The method was validated for PESs of small molecules,  $\text{CH}_4$  and  $\text{H}_3\text{O}^+$  and for 12-atom *N*-methyl acetamide. Here, We apply our  $\Delta$ -learning approach to 15-atom AcAc,  $\text{C}_5\text{H}_8\text{O}_2$ , and we use a similar local CCSD(T) method to the one used by Meuwly and co-workers.

The approach is to construct a high-level, CCSD(T) PES starting from a lower level, MP2 one using a correction which is a fit to a small number of high-level *ab initio* energies. Explicitly, the corrected

high-level PES, denoted  $V_{LL \rightarrow CC}$  is given by

$$V_{LL \rightarrow CC} = V_{LL} + \Delta V_{CC-LL}, \quad (1)$$

where  $V_{LL}$  is the lower-level PES and  $\Delta V_{CC-LL}$  is the correction PES. In the present application to AcAc we we calculated 2151 LCCSD(T)-F12 energies<sup>23</sup> and performed training on a subset of these ranging in size from 430 to 1935. (By comparison,  $V_{LL}$  was fit using a data size of 250 884.) The details of the selection of these configurations and fit details are given below in the Methods section. However, for assessing the results shown next, we note that the  $\Delta V_{CC-LL}$  fit uses only 85 PIPs and thus that many linear coefficients. This is a very small basis; however, it does permit training (without overfitting) with small datasets.

## Results

### Summary of $\Delta$ -ML performance with respect to training size

Numerous metrics of the performance of the  $\Delta$ -ML approach are given in Table 1. Beginning with training and testing errors of the  $\Delta V_{CC-LL}$  PESs using training sets of different sizes, we note that the testing set consists of points not used for training. It can be seen that the testing error increases monotonically as the number of training points decreases, due to smaller coverage by the training data. However, this increase in the testing error is relatively small.

**Table 1.** Indicated RMS errors of the  $\Delta V_{CC-LL}$  PESs using training sets of different sizes,  $N$ . Training and testing RMSs refer to energies, the barrier height is for symmetric H-transfer, the RMS errors in internuclear distances are given for the global minimum (GM) and H-atom transfer saddle point (SP). The mean absolute errors (MAE) are given for harmonic frequencies relative to benchmark LCCSD(T) results. Energies and frequencies are in  $\text{cm}^{-1}$ , and distances in  $\text{\AA}$ .

	$N=1935$	$N=1075$	$N=717$	$N=430$	$V_{LL}$
Training RMS	99.6	94.7	98.8	79.3	-
Testing RMS	107.5	113.7	123.0	155.9	-
Barrier height	1218	1217	1219	1219	745
RMS (GM geom)	0.0081	0.0076	0.0078	0.0070	0.0115
RMS (SP geom)	0.0041	0.0041	0.0041	0.0036	0.0026
MAE (GM freq)	12.2	12.1	13.3	13.7	17.3
MAE (SP freq)	24.7	24.8	26.2	25.9	35.6

Next we consider the equilibrium geometries and normal mode frequencies of both the global minimum (GM) and the saddle point to H transfer (SP), as well as the barrier height. For geometries, we computed the root-mean-square (RMS) difference between the 105 internuclear distances from the PES and direct LCCSD(T)-F12 optimized geometries. For harmonic frequencies, we calculated the mean absolute error (MAE) by comparing frequencies from PESs with direct LCCSD(T)-F12 ones. All these are listed in Table 1 for four PESs with different training sets as well as the low-level MP2 PES.

We get excellent agreement for the geometries: in all four  $\Delta$ -ML PESs, the RMS differences of the 105 internuclear distances between PES and direct LCCSD(T) geometries are around 0.008 and 0.004  $\text{\AA}$  for GM and SP, respectively; while the RMS differences between  $V_{LL}$  and LCCSD(T) geometries are 0.0115 and 0.0026  $\text{\AA}$  for GM and SP. Therefore the geometry of GM is slightly improved using the  $\Delta$ -ML

approach, and the SP geometry is still in good agreement with the LCCSD(T)-F12 one despite slightly increased RMS difference (only 0.0014 Å). A plot of  $V_{LL \rightarrow CC}$  inter-nuclear distances vs direct *ab initio* ones is shown in Fig. 1. It is perhaps worth noting that the largest distances (nearly 7 Å) are between the H atoms in the two methyl rotors shown in Fig. 3 below.

The barrier height of the H-transfer motion on all 4 corrected PESs, each based on a different training set, are around  $1218 \text{ cm}^{-1}$  (3.49 kcal/mol), in excellent agreement with the direct LCCSD(T)-F12 value of  $1234 \text{ cm}^{-1}$  (3.54 kcal/mol). The best estimate of this barrier height is  $1148 \text{ cm}^{-1}$  (3.29 kcal/mol), based on CCSD(T)-F12/aug-cc-pVTZ single point calculations at the LCCSD(T)-optimized geometries. So the  $\Delta$ -ML PES slightly overestimates the barrier height; nevertheless, it is a significant improvement over the MP2 PES<sup>13</sup>, which has a barrier height of  $745 \text{ cm}^{-1}$  (2.13 kcal/mol).

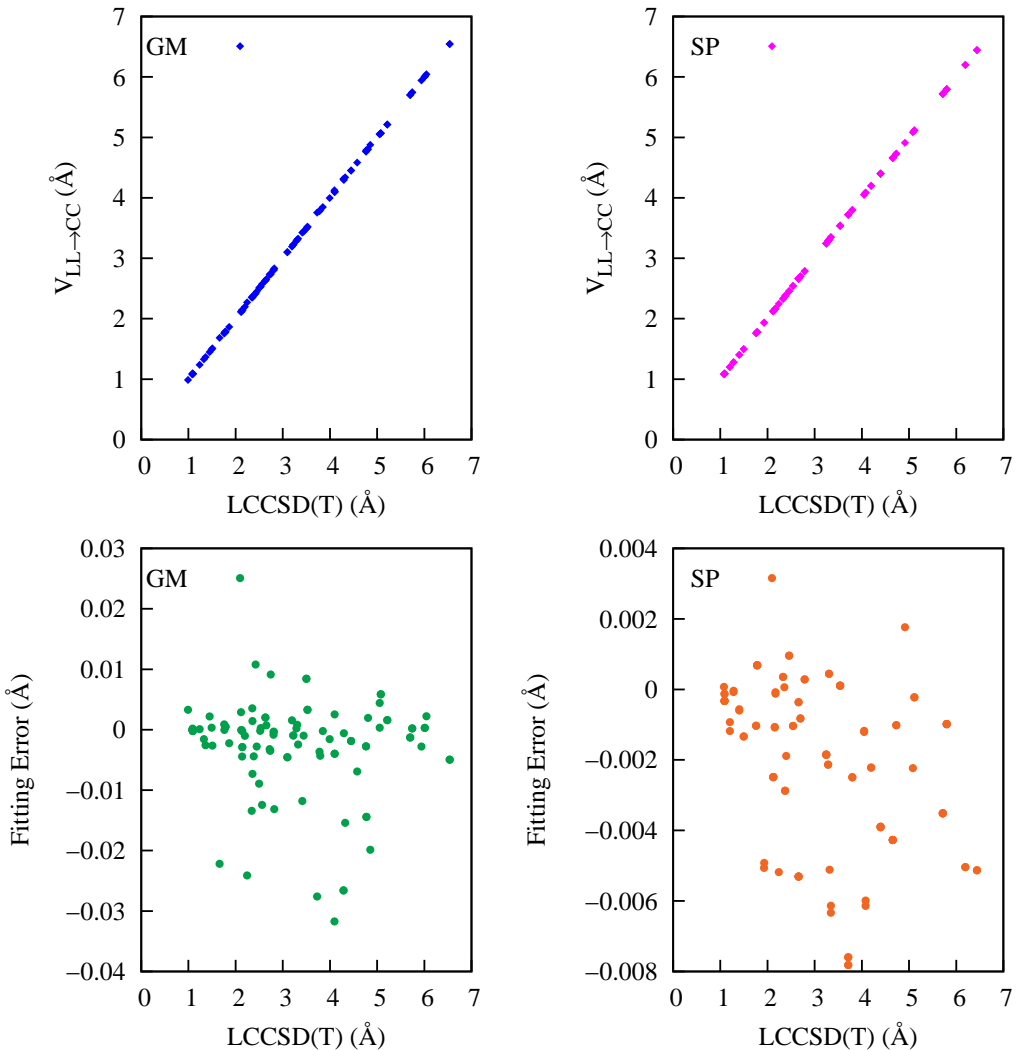


**Figure 1.** Plot of fitting errors in inter-nuclear distances. The upper panel represents the plot of  $\Delta$ -ML PES distance vs direct LCCSD(T) distance and the lower panel represents the fitting error at each distance.

The energies of 7 low-lying stationary points (including the GM and SP) are shown in Table 2. TS(T)-I/II/III are three saddle points with respect to the torsion of the two methyl rotors, and TS(HT)-I/II are two higher-order saddle points with imaginary frequencies in both H-transfer motion and the methyl torsion. In nearly all cases, the energies of the stationary points are better captured by the  $V_{LL \rightarrow CC}$  PESs than by

the  $V_{LL}$  one.

**Table 2.** Energies relative to the global minimum, GM, (in  $\text{cm}^{-1}$ ) of the 7 stationary points using indicated methods. The numbers in parentheses for the two  $\Delta$ -ML PESs refer to the size of training data.

Stationary points	LCCSD(T)	$V_{LL \rightarrow CC}$ (1935)	$V_{LL \rightarrow CC}$ (430)	$V_{LL}$
GM	0	0	0	0
SP	1234	1218	1219	745
TS(T)-I	123 <sup>a</sup>	165	154	160
TS(T)-II	488 <sup>a</sup>	477	481	399
TS(T)-III	581 <sup>a</sup>	627	623	541
TS(HT)-I	1434 <sup>a</sup>	1299	1306	820
TS(HT)-II	1645 <sup>a</sup>	1359	1374	864

<sup>a</sup> LCCSD(T)-F12 calculations at MP2-optimized geometries

The harmonic frequencies of the global minimum and saddle point from the MP2 PES ( $V_{LL}$ ), the corrected PES ( $V_{LL \rightarrow CC}$ ) using 1935 training points, and direct LCCSD(T)-F12 calculations are listed in Table 3. For most of the modes, the differences between  $V_{LL}$  and  $V_{LL \rightarrow CC}$  frequencies are small, but for mode 32 of GM (OH stretch) and the imaginary-frequency mode of SP, the improvement of the  $\Delta$ -ML PES is significant. Again, the 4  $\Delta$ -ML PESs based on different training sets achieved similar MAE in frequencies (around  $13 \text{ cm}^{-1}$  for GM and  $25 \text{ cm}^{-1}$  for SP, see Table 1), and that is a significant improvement over the low-level PES, which has MAEs of  $17.3$  and  $35.6 \text{ cm}^{-1}$  for GM and SP, respectively.

These results show that the  $\Delta$ -ML approach indeed improves the PES and brings it closer to coupled-cluster level of accuracy. This approach significantly improves the barrier height of H transfer, moderately improves the harmonic frequencies of GM and SP, and slightly improves the optimized geometries of GM and SP. More importantly, even with a training set as small as 430 points, the corresponding  $V_{LL \rightarrow CC}$  PES is almost as good as the one fitted to 1935 points. Nevertheless, the fit using 1935 points is still our best one in terms of coverage of configurations and testing error, and so the results shown next are based on this fit.

### Diffusion Monte Carlo results for the H-atom Transfer Tunneling Splitting

The zero-point energy of the corrected PES using 10 DMC calculations is  $26741 \pm 7 \text{ cm}^{-1}$ , while the energy of the excited state for the H-transfer motion from 10 fixed-node DMC calculations is  $26773 \pm 10 \text{ cm}^{-1}$ ; therefore the tunneling splitting is  $32 \text{ cm}^{-1}$ . As a comparison, the splitting we obtained using the MP2-based PES (i.e.,  $V_{LL}$ ) is  $160 \text{ cm}^{-1}$ . Such a significant decrease in the tunneling splitting is expected because the barrier height of the  $V_{LL \rightarrow CC}$ ,  $1218 \text{ cm}^{-1}$ , is significantly higher than the barrier height from the  $V_{LL}$ ,  $745 \text{ cm}^{-1}$ .

We also performed the DMC calculations for the singly deuterated isotopologue of AcAc, but the energies of the ground state and excited state are too close so that the splitting is smaller than the uncertainty in the DMC calculations. Therefore, we could not obtain a reliable estimate of the tunneling splitting for the deuterated AcAc using DMC.

### H and D-atom Transfer Tunneling Splittings Using the $Q_{im}$ path

We also applied the approximate 1d approach to obtain the tunneling splittings described above. The two mass-scaled 1d potentials (one for H and the other for D-transfer) are shown in Fig. 2.

**Table 3.** Harmonic frequencies (in  $\text{cm}^{-1}$ ) of the global minimum and H-transfer saddle point of acetylacetone from the indicated sources. Training was done with 1935 LCCSD(T) energies.

mode	Global Minimum			Saddle Point		
	LCCSD(T)	$\text{V}_{LL \rightarrow CC}$	$\text{V}_{LL}$	LCCSD(T)	$\text{V}_{LL \rightarrow CC}$	$\text{V}_{LL}$
1	113	97	97	$1278i$	$1082i$	$921i$
2	133	120	119	100	57	53
3	169	157	153	121	62	57
4	197	191	189	165	159	156
5	236	227	229	198	197	198
6	372	359	364	289	286	285
7	392	389	390	412	416	417
8	505	502	507	537	530	531
9	554	570	567	540	540	539
10	643	652	650	578	589	580
11	654	657	656	661	654	645
12	793	801	803	767	739	740
13	919	881	921	781	751	756
14	942	912	936	949	947	953
15	951	934	942	992	981	979
16	1010	1005	1014	1035	1032	1039
17	1040	1044	1048	1037	1039	1043
18	1050	1052	1058	1054	1059	1060
19	1072	1069	1071	1067	1060	1062
20	1192	1192	1200	1195	1182	1189
21	1276	1270	1290	1308	1250	1223
22	1393	1377	1384	1341	1341	1347
23	1405	1404	1399	1406	1401	1409
24	1424	1433	1433	1413	1418	1422
25	1462	1450	1470	1481	1490	1496
26	1480	1486	1494	1487	1491	1496
27	1483	1489	1497	1488	1494	1500
28	1488	1499	1505	1491	1496	1502
29	1502	1508	1512	1569	1560	1567
30	1670	1662	1655	1613	1617	1629
31	1709	1705	1704	1624	1648	1670
32	3047	3058	2855	1904	1744	1685
33	3052	3080	3095	3054	3058	3098
34	3118	3122	3099	3057	3079	3099
35	3122	3170	3178	3130	3179	3190
36	3157	3178	3187	3132	3180	3190
37	3165	3203	3208	3154	3196	3207
38	3220	3210	3218	3156	3197	3208
39	3257	3248	3258	3241	3273	3282

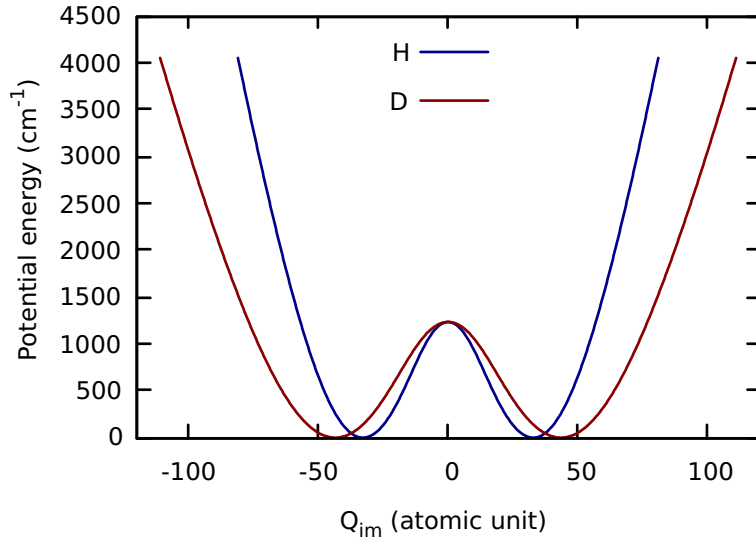


**Figure 2.** One-dimensional  $V(Q_{im})$  path for H and D transfer in AcAc. The barrier heights have been “morphed” to agree with LCCSD(T)-F12 value.

These potentials were, at first, obtained with the two methyl rotors restricted to their structures at the saddle-point, since it is not practical to get correct relaxation of these using the  $Q_{im}$  approach. Thus, the barrier height from these not-fully relaxed potentials are  $179\text{ cm}^{-1}$  less than the LCCSD(T) value. So, a small scaling (“morphing”) of these potentials was done to produce the correct barrier height.

Using this 1d approach, the ground-state tunneling splittings are  $37.9$  and  $8.2\text{ cm}^{-1}$  for H and D, respectively; the H-splitting is in reasonably good agreement with the  $32\text{ cm}^{-1}$  obtained from the DMC calculation, and the D-splitting is also consistent with the fact that it is smaller than the uncertainty of the DMC calculations.

## Discussion

It is clearly seen that the  $\Delta$ -ML approach can indeed bring the PES closer to the CCSD(T) level of accuracy, especially as applied to the barrier height of the H-atom transfer. Of course these improvements are not achieved without extra cost.

First, there is an extra cost to compute the LCCSD(T)-F12 energies for 2151 configurations. A single-point calculation of the energy takes about 30 minutes using 12 cores of the 2.4 GHz Intel Xeon processor, and all the 2151 points can be completed within one week using 7 nodes for these computations. As we have shown above, far fewer points can be used to obtain a high-quality correction PES. So, this cost is affordable and minor.

What is more important is the extra cost in the PES. In the  $\Delta$ -ML approach, the extra cost is the calculation of the energy correction,  $\Delta V_{CC-LL}$ . For AcAc, the  $\Delta V_{CC-LL}$  PES uses maximum polynomial order of 2 and it costs about 10% of the  $V_{LL}$  PES. So this additional cost is also a small price to pay for bringing the accuracy of the PES, especially the barrier height for the H-atom transfer, to near the coupled-cluster level.

The success in bringing an MP2-based full-dimensional PES for 15-atom acetylacetone to the coupled-cluster quality is very encouraging. Given that a small number (around 500 to 2000) of coupled-cluster energies were needed for the correction makes it clear that the approach should be readily applicable to

molecules with more than 10 atoms. The coupled-cluster approach used was the relatively efficient local method LCCSD(T) available in the 2015 version of Molpro we use.<sup>24</sup>

We think it is also worth commenting on the current  $\Delta$ -ML approach and the recent application of transfer learning (TL) by Meuwly and co-workers<sup>14</sup> to MP2-based PESs for AcAc. The MP2-based PES we reported used a slightly extended database of MP2 energies and gradients from that group. Thus, the PES we reported is not the same as the earlier one. However, they are similar, e.g., the H-atom transfer barrier heights are 2.13 and 2.17 kcal/mol for the PIP PES and the NN PES, respectively. These are in very good agreement with the direct MP2 result of 2.18 kcal/mol.

Several TL NN models, based on random training data sets (PNO-LCCSD(T) energies) of different sizes, were considered by Meuwly and co-workers.<sup>14</sup> In Table 3 of that paper, results both from a single TL NN model and from an average of several TL NN models were given at the optimized geometries of each model. A TL-NN model gave a barrier height of 0.92 kcal/mole using 100 high-level energies, 2.4 kcal/mol from a single TL-NN model, 1.80 kcal/mol averaged from several TL-NN models with 1000 energies, and 2.66 kcal/mol from a single TL-NN model using 5000 energies. Barrier heights of 3.31 and 3.32 kcal/mol were obtained with a single and multiple TL-NN models using 15 000 energies; these are in excellent agreement with the benchmark barrier height of 3.25 kcal/mol. From these results two apparent conclusions emerge. The first is that the TL-NN may produce a worse result, i.e., a lower barrier height, than the original NN PES, and the second is that roughly 15 000 high-level energies are needed to obtain a TL-NN PES with an accurate barrier height. (These authors did note some improvement in the TL-NN model using 1000 energies by the addition of 100 energies along the minimum energy path, i.e., the barrier height went from 1.8 to 2.72 kcal/mol.)

Thus, based on the above it appears our  $\Delta$ -ML approach performs significantly better than the TL one for this example. This is of course an “early-days” conclusion. However, unlike the TL-NN approach, the  $\Delta$ -ML approach we applied does not produce worse results than the low-level PES. We attribute this to the fact that the difference potential is “small” relative to the low-level and high-level potentials. If this is not true (and this can be checked of course) then the current approach would probably require a larger database of high-level energies to achieve a satisfactory result.

## Methods

### Fragmented PIP Fitting

In the permutationally invariant polynomial (PIP) approach to fitting,<sup>25</sup> the potential  $V$  is represented in compact notation by

$$V(\mathbf{x}) = \sum_{i=1}^{n_p} c_i p_i(\mathbf{x}), \quad (2)$$

where  $c_i$  are linear coefficients,  $p_i$  are PIPs,  $n_p$  is the total number of polynomials for a given maximum polynomial order and  $\mathbf{x}$  are Morse variables. For example,  $x_{\alpha\beta}$  is given by  $\exp(-r_{\alpha\beta}/\lambda)$ , where  $r_{\alpha\beta}$  is the internuclear distance between atoms  $\alpha$  and  $\beta$ . The range (hyper) parameter is commonly chosen to be equal to roughly 2 bohr. The linear coefficients are obtained using standard least squares fits to large data sets of electronic energies (and, for large molecules, gradients as well) at “scattered” geometries.

For molecules of more than ten atoms, the size of the PIP basis can become a computational bottleneck. This size depends in a complicated and non-linear way with respect to the maximum polynomial order, the number of Morse variables, and the order of the symmetric group.<sup>25</sup> While we have been able to use a full PIP basis even for 15-atom tropolone<sup>12</sup> and AcAc<sup>13</sup>, we have shown that the fragmented PIP, which can be applied to larger molecules, performs very well and runs faster than the full PIP basis.

The fragmented PIP basis is obtained by fragmenting a molecule into groups of atoms. A PIP basis for each group can be calculated rapidly and then combined with those of other groups to provide a compact and still precise representation of the PES.<sup>9</sup> Indeed this has been verified for *N*-methyl acetamide,<sup>9,10</sup> tropolone,<sup>12</sup> and AcAc.<sup>13</sup> Note that these PESs use the most recent software that include gradients in the fit and produces gradients on output.<sup>26-28</sup>

The relevant details of this approach for AcAc are as follows. AcAc was cut into four fragments and PIP bases with maximum polynomial order of three were obtained for each fragment. The details of this approach have been described previously,<sup>9,10,27</sup> as have the specific details for AcAc.<sup>13</sup> The fragmentation scheme was denoted by 4-(9,11,11,8), where the numbers in parentheses represent the number of atoms in each fragment. The atom labeling for the AcAc potential is given in Fig. 3. The permutational symmetries for these atom group is as follows: {1, 1, 1, 1, 1, 1, 1, 1, 1}, i.e., no symmetry, for atoms {1, 2, 3, 4, 5, 6, 10, 11, 12}; {3, 1, 1, 1, 1, 1, 1, 1} for atoms {13, 14, 15, 1, 2, 3, 4, 5, 10, 11, 12}; {3, 1, 1, 1, 1, 1, 1, 1} for atoms {7, 8, 9, 1, 2, 3, 4, 5, 6, 10, 11}; and {3, 3, 1, 1} for atoms {7, 8, 9, 13, 14, 15, 6, 12}. With this reduced symmetry we obtain a symmetric double well and perfect equivalence of the three H atoms in the two methyl rotors.

The PES obtained with this fragmentation scheme had a weighted RMS fitting error of 22 cm<sup>-1</sup> for energies and 16 cm<sup>-1</sup>/bohr for gradients. The performance of this PES against direct MP2 calculations was examined in detail in the previous paper.<sup>13</sup> In particular, the barrier for the symmetric H-atom transfer is 745 cm<sup>-1</sup> on the PES in excellent agreement with the direct MP2 value of 763 cm<sup>-1</sup>. However, as noted already this is significantly less than the CCSD(T) value of around 1150 cm<sup>-1</sup>.<sup>15</sup> Correcting this error on the MP2-based PES is a major goal of  $\Delta$ -Machine Learned method, which is described briefly next.

## The data base and potential energy surface fits

The database of MP2 points has been described previously.<sup>13</sup> It consists of *ab initio* energies and gradients at 5454 different molecular configurations, using MP2/aug-cc-pVTZ level of theory. Of these configurations, as already anticipated, 5000 were provided by the authors of ref. 14, while an additional 454 configurations were generated through grids of points near the transition state to H transfer and near the global minimum, as well as by running *ab initio* molecular dynamics trajectories at an energy of 4000 cm<sup>-1</sup>. At these configurations, energies and full gradients were obtained and used in the database, for a total data size of 250 884.

The database used to calculate the difference potential  $\Delta V_{CC-LL}$  was generated by choosing 2151 geometries from the MP2 data base and calculating the LCCSD(T)-F12 energies at these geometries using Molpro.<sup>24</sup> The points chosen included the 1100 geometries nearest to the global minimum (denoted GM) and the saddle point for the H-atom transfer (denoted SP), and another 1051 taken by choosing a random integer that indicated their position on a list, discarding choices whose energies were more than 30,000 cm<sup>-1</sup>, and stopping the selection when the requisite number of choices had been made. This small number of points is chosen to produce a new PES with a barrier for H-atom transfer that is much closer to the direct LCCSD(T) one than the MP2 one, which as noted is more than 1 kcal/mol low.

Figures 4(a) and (b) show histograms of the MP2 data base and the difference energies obtained from the LCCSD(T)-F12 energies. The MP2 energies are relative to the MP2 global minimum and the LCCSD(T) ones are also relative to that GM. The MP2 data base has peaks near the GM and SP and a broad distribution up to an energy of about 40 000 cm<sup>-1</sup>. The difference data base shows a peak near zero energy difference with a distribution stretching from approximately -1500 to 800 cm<sup>-1</sup>. Of course, these 1d histograms do not capture the correlation between the two energy groups; this correlation is shown in Figure 4(c). Clearly, there isn't a simple correlation. The largest energy differences are for geometries whose MP2 energies are between 10 000 and 20 000 cm<sup>-1</sup> whereas small difference are seen for MP2

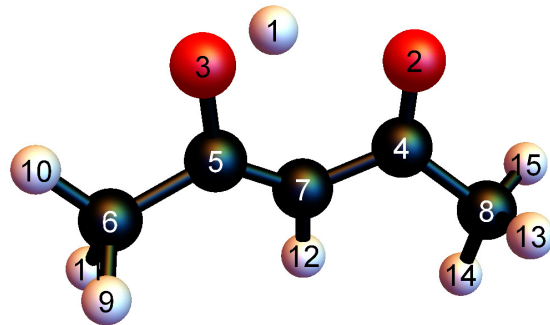
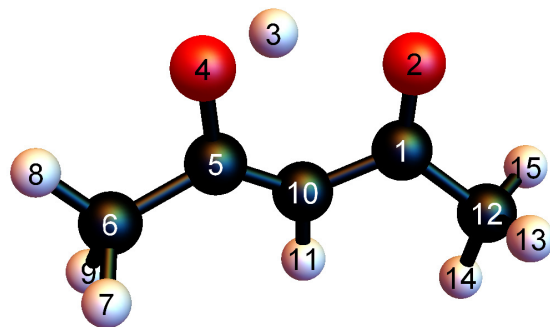


**Figure 3.** Numbering schemes used in the PES fits. (top) for the 4-(9,11,11,8) fit. (bottom) for the difference fit, of symmetry 1,2,5,7.

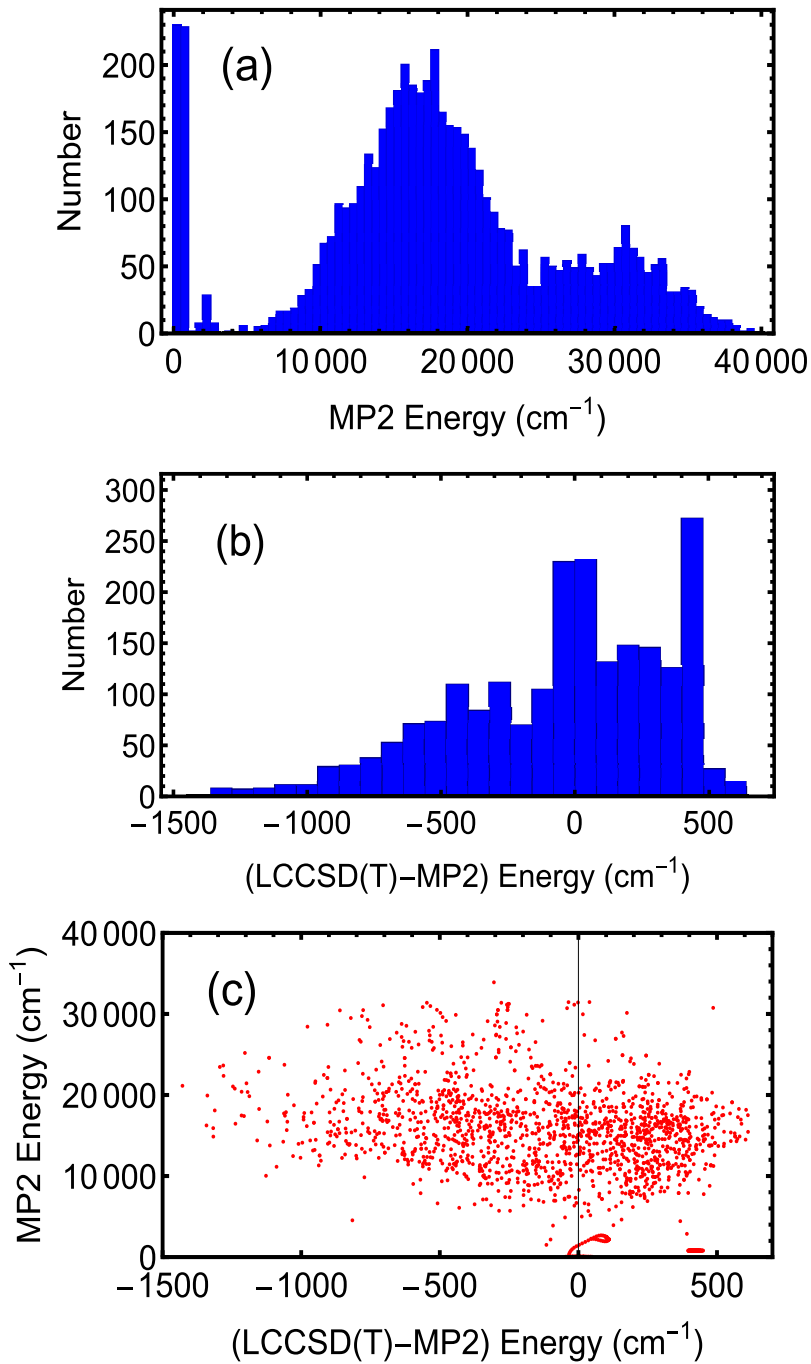


**Figure 4.** Energies of MP2 and difference fits. (a) Histogram of MP2 energies for 4-(9,11,11,8) fit. The bin size is  $500 \text{ cm}^{-1}$ . (b) Histogram of difference between the LCCSD(T) and MP2 energies used in the  $\Delta V_{CC-LL}$  fit. The bin size is  $80 \text{ cm}^{-1}$ . (c) Correlation between energies histogram in (a) and (b).

energies as large as  $30\,000\text{ cm}^{-1}$ .

The distributions of configurations where MP2 and LCCSD(T) calculations were done are shown in Fig. 5 and 6, respectively. The plot axes show the two OH distances, where O is the transferring H atom. Note that other distances are changing as well, and this is indicated schematically by the structures shown in the top panel. As seen, both sets are sparse although dispersed.

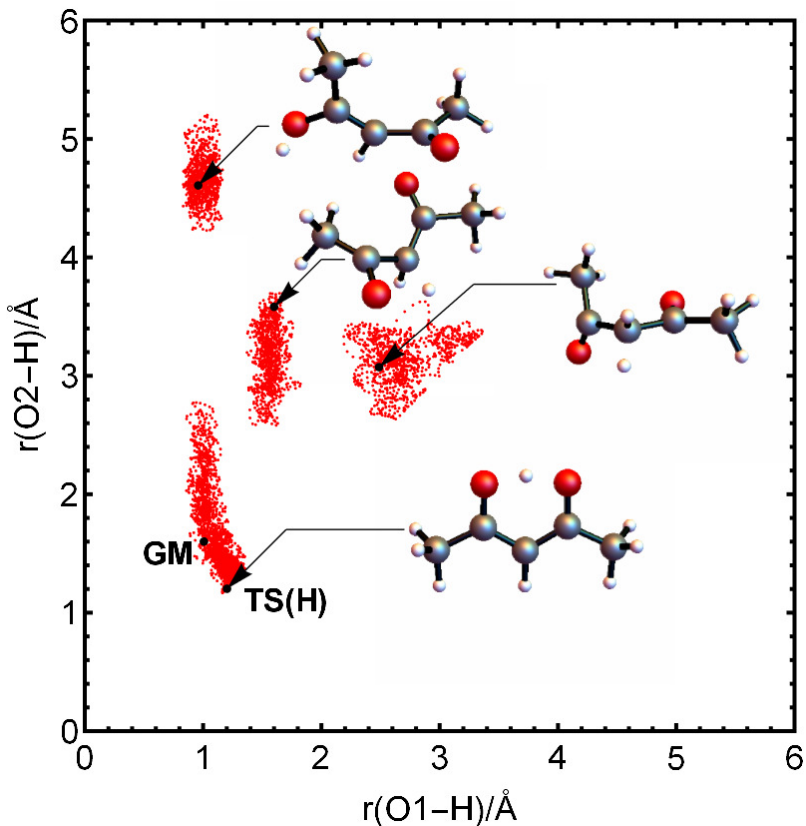


**Figure 5.** Scatter plots of distribution of points: MP2 points with representative structures.

In addition to the LCCSD(T)-F12 energies calculated for the PES data base, we performed two benchmark calculations at the global minimum and at the saddle point for H-atom transfer. These two calculations found the optimum geometry and energy and determined as well the harmonic vibrational frequencies and normal coordinates. While the LCCSD(T)-F12 calculations for just the energy at a single geometry took approximately 30 minutes using 12 cores of the 2.4 GHz Intel Xeon processors, the full optimization and frequency calculations took on the order of 73 days using the same number of processors. This computational cost certainly underscores the infeasibility of doing even approximate LCCSD(T) calculations for an AcAc PES.

The fragmented potential energy fit we used for the MP2 data base has been described in detail previously,<sup>13</sup> and briefly above.

The fit to the difference potential has to take account of the small data set, i.e., a maximum of 2151 energies. Therefore, the number of terms in the PIP basis has to be significantly less than this number to avoid overfitting. With this in mind we used a PIP basis of maximum polynomial order of 2 and a symmetry designation of 1,2,5,7, meaning that the 2 oxygens were allowed to permute, the 5 carbons were allowed to permute, and 7 of the hydrogens were allowed to permute. The last hydrogen, which was

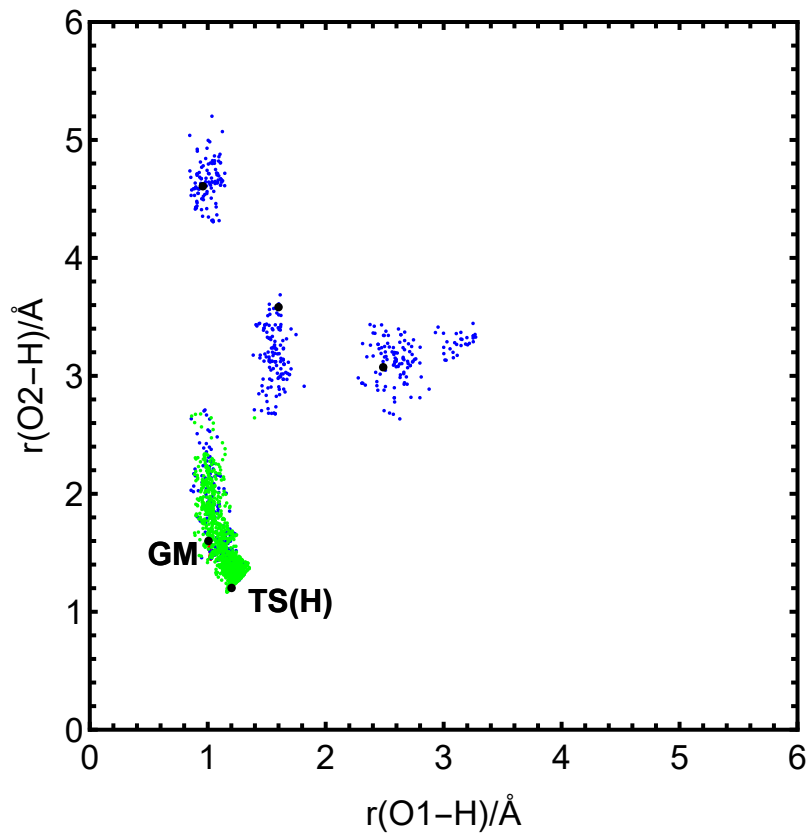


**Figure 6.** LCCSD(T) points using all points near the GM (green) and other random scattered points (blue), explained in the text.

not allowed to permute with the other hydrogens, was the one that is transferred between the two oxygen atoms. The numbering scheme for this fit is shown in Fig. 3(b). This basis contains just 85 PIPs and thus 85 linear coefficients to be determined by standard least-squares regression.

This is the smallest PIP we have ever used, and the “bonus” is that we can examine small training data sets without concerns about overfitting. We do note that the RMS fitting error for the full database of 2151 energies is  $95 \text{ cm}^{-1}$  (0.27 kcal/mol).

## Diffusion Monte Carlo Calculations

Diffusion Monte Carlo (DMC) calculations were employed to compute the ground-state tunneling splitting of AcAc. Specifically, the simple unbiased algorithm,<sup>29,30</sup> was used to calculate the ground-state energy, while DMC with fixed-node approximation<sup>31</sup> was used to calculate the energy of the excited state with respect to the H-transfer motion.

In the simple unbiased algorithm, which we use, an ensemble of random walkers is used to represent the nuclear wavefunction of the molecule. At each step, a random displacement in each degree of freedom is assigned to each walker, and this walker may remain alive (and may give birth to a new walker) or be killed by comparing its potential energy,  $E_i$ , with a reference energy,  $E_r$ . For the ground state, the probability of birth or death is given as:

$$P_{\text{birth}} = \exp [-(E_i - E_r)\Delta\tau] - 1 \quad (E_i < E_r) \quad (3)$$

$$P_{\text{death}} = 1 - \exp [-(E_i - E_r)\Delta\tau] \quad (E_i > E_r), \quad (4)$$

where  $\Delta\tau$  is the step size in imaginary time. In fixed-node approximation for excited states, in addition to the process described above, any walker that crosses a node is instantly killed. In most cases the node is unknown in Cartesian coordinates, but for certain modes such as H-transfer in symmetric double-well, a very reasonable approximation can be made for the node as described in detail below.

After removing all dead walkers, the reference energy is updated using the equation

$$E_r(\tau) = \langle V(\tau) \rangle - \alpha \frac{N(\tau) - N(0)}{N(0)}, \quad (5)$$

where  $\tau$  is the imaginary time;  $\langle V(\tau) \rangle$  is the average potential over all the walkers that are alive;  $N(\tau)$  is the number of live walkers at time  $\tau$ ;  $\alpha$  is a parameter that can control the fluctuations in the number of walkers and the reference energy. Finally, the average of the reference energy over the imaginary time gives an estimate of ZPE (or the energy of the excited state in a fixed-node calculation).

For AcAc, DMC calculations were performed in Cartesian coordinates in full dimensionality. For fixed-node calculation, we assume that the node is  $r_{\text{OH}2} = r_{\text{OH}4}$  (using the numbering scheme shown in the top panel of Figure 3). Initially, the H atom is closer to one O (say O4), so if  $r_{\text{OH}4}$  of a walker becomes larger than  $r_{\text{OH}2}$ , that walker crosses the node and would be instantly removed. An additional correction was made for the excited state by taking recrossing into consideration.<sup>31</sup>

Ten DMC simulations were performed for each state, and in each simulation, 30000 walkers were equilibrated for 5000 steps, and then were propagated for 50000 steps to compute the energy, with a step size of 5.0 au. In these simulations,  $\sim 10^{10}$  potential energy evaluations are required; clearly these cannot be done without an efficient PES.

## One-dimensional Tunneling Calculation

The 1d approach to calculate the tunneling splitting has been described in detail previously.<sup>32</sup> It was used in our previous work on AcAc based on the MP2 PES (PES<sub>LL</sub>).<sup>13</sup> Briefly, a 1d potential, denoted  $V(Q_{im})$ ,

which is the minimum energy path as a function of the imaginary-frequency mode ( $Q_{im}$ ) of the H-transfer saddle point, was obtained by optimizing all the other coordinates at fixed  $Q_{im}$  values using the  $V_{LL \rightarrow CC}$  PES except the methyl rotors, which cannot be described using rectilinear normal coordinates. These are held fixed at the saddle point values all the way along the path. Due to fixed methyl orientation and fitting error, the barrier height of this 1d  $Q_{im}$  path is  $1055 \text{ cm}^{-1}$  and it is  $179 \text{ cm}^{-1}$  lower than the LCCSD(T) value. Therefore, we “morphed” this 1d potential using the same strategy as described previously<sup>13</sup> so that it gives the correct barrier height ( $1234 \text{ cm}^{-1}$ ).

The splittings are obtained simply using 1d-DVR calculations<sup>33</sup> of the energies of the ground and first excited states on the morphed  $V(Q_{im})$  paths, and thus the splitting. We note that this approach was applied to obtain the tunneling splittings of H-atom and D-atom transfer in malonaldehyde.<sup>32</sup> The results were within roughly 10 percent of the rigorous diffusion Monte Carlo splittings.

## References

1. Bowman, J. M., Czakó, G. & Fu, B. High-dimensional ab initio potential energy surfaces for reaction dynamics calculations. *Phys. Chem. Chem. Phys.* **13**, 8094–8111 (2011).
2. Qu, C., Yu, Q. & Bowman, J. M. Permutationally invariant potential energy surfaces. *Annu. Rev. Phys. Chem.* **69**, 6.1–6.25 (2018).
3. Fu, B. & Zhang, D. H. Ab initio potential energy surfaces and quantum dynamics for polyatomic bimolecular reactions. *J. Chem. Theory Comput.* **14**, 2289–2303 (2018).
4. Jiang, B., Li, J. & Guo, H. High-fidelity potential energy surfaces for gas-phase and gas-surface scattering processes from machine learning. *J. Phys. Chem. Lett.* **11**, 5120–5131 (2020).
5. Qu, C. & Bowman, J. M. An ab initio potential energy surface for the formic acid dimer: Zero-point energy, selected anharmonic fundamental energies, and ground-state tunneling splitting calculated in relaxed 1–4-mode subspaces. *Phys. Chem. Chem. Phys.* **18**, 24835–24840 (2016).
6. Papp, D., Tajti, V., Győri, T. & Czakó, G. Theory finally agrees with experiment for the dynamics of the  $\text{Cl} + \text{C}_2\text{H}_6$  reaction. *J. Phys. Chem. Lett.* **11**, 4762–4767 (2020).
7. Fu, Y.-L. *et al.* Collision-induced and complex-mediated roaming dynamics in the  $\text{H} + \text{C}_2\text{H}_4 \rightarrow \text{H}_2 + \text{C}_2\text{H}_3$  reaction. *Chem. Sci.* **11**, 2148–2154 (2020).
8. Lu, D., Behler, J. & Li, J. Accurate global potential energy surfaces for the  $\text{H} + \text{CH}_3\text{OH}$  reaction by neural network fitting with permutation invariance. *J. Phys. Chem. A* **124**, 5737–5745 (2020).
9. Qu, C. & Bowman, J. M. A fragmented, permutationally invariant polynomial approach for potential energy surfaces of large molecules: Application to N-methyl acetamide. *J. Chem. Phys.* **150**, 141101 (2019).
10. Nandi, A., Qu, C. & Bowman, J. M. Full and fragmented permutationally invariant polynomial potential energy surfaces for *trans* and *cis* N-methyl acetamide and isomerization saddle points. *J. Chem. Phys.* **151**, 084306 (2019).
11. Conte, R., Houston, P. L., Qu, C., Li, J. & Bowman, J. M. Full-dimensional, ab initio potential energy surface for glycine with characterization of stationary points and zero-point energy calculations by means of diffusion monte carlo and semiclassical dynamics. *J. Chem. Phys.* **153**, 244301 (2020).
12. Houston, P. L., Conte, R., Qu, C. & Bowman, J. M. Permutationally invariant polynomial potential energy surfaces for tropolone and H and D atom tunneling dynamics. *J. Chem. Phys.* **153**, 024107 (2020).
13. Qu, C., Conte, R., Houston, P. L. & Bowman, J. M. Full-dimensional potential energy surface for acetylacetone and tunneling splittings. *Phys. Chem. Chem. Phys.* (in press) (2021).
14. Käser, S., Unke, O. & Meuwly, M. Reactive dynamics and spectroscopy of hydrogen transfer from neural network-based reactive potential energy surfaces. *New J. Phys.* **22**, 055002 (2020).
15. Howard, D. L., Kjaergaard, H. G., Huang, J. & Meuwly, M. Infrared and near-infrared spectroscopy of acetylacetone and hexafluoroacetylacetone. *J. Phys. Chem. A* **119**, 7980–7990 (2015).
16. Pan, S. J. & Yang, Q. A survey on transfer learning. *IEEE Trans. Knowl. Data Eng.* **22**, 1345–1359 (2010).
17. Smith, J. S. *et al.* Approaching coupled cluster accuracy with a general-purpose neural network potential through transfer learning. *Nat. Commun.* **10**, 2903–2906 (2019).

18. Chmiela, S., Sauceda, H. E., Müller, K.-R. & Tkatchenko, A. Towards exact molecular dynamics simulations with machine-learned force fields. *Nat. Commun.* **9**, 3887 (2018).
19. Sauceda, H. E., Chmiela, S., Poltavsky, I., Müller, K.-R. & Tkatchenko, A. Molecular force fields with gradient-domain machine learning: Construction and application to dynamics of small molecules with coupled cluster forces. *J. Chem. Phys.* **150**, 114102 (2019).
20. Stöhr, M., Medrano Sandonas, L. & Tkatchenko, A. Accurate many-body repulsive potentials for density-functional tight binding from deep tensor neural networks. *J. Phys. Chem. Lett.* **11**, 6835–6843 (2020).
21. Ramakrishnan, R., Dral, P. O., Rupp, M. & von Lilienfeld, O. A. Big data meets quantum chemistry approximations: The  $\Delta$ -machine learning approach. *J. Chem. Theory Comput.* **11**, 2087–2096 (2015).
22. Nandi, A., Qu, C., Houston, P. L., Conte, R. & Bowman, J. M.  $\Delta$ -machine learning for potential energy surfaces: A PIP approach to bring a DFT-based PES to CCSD(T) level of theory. *J. Chem. Phys.* **154**, 051102 (2021).
23. Adler, T. B. & Werner, H.-J. Local explicitly correlated coupled-cluster methods: Efficient removal of the basis set incompleteness and domain errors. *J. Chem. Phys.* **130**, 241101 (2009).
24. Werner, H.-J., Knowles, P. J., Knizia, G., Manby, F. R. & Schütz, M. Molpro, version 2015.1, a package of ab initio programs (2015). See <http://www.molpro.net>.
25. Braams, B. J. & Bowman, J. M. Permutationally invariant potential energy surfaces in high dimensionality. *Int. Rev. Phys. Chem.* **28**, 577–606 (2009).
26. Nandi, A., Qu, C. & Bowman, J. M. Using gradients in permutationally invariant polynomial potential fitting: A demonstration for  $\text{CH}_4$  using as few as 100 configurations. *J. Chem. Theory Comput.* **15**, 2826–2835 (2019).
27. Conte, R., Qu, C., Houston, P. L. & Bowman, J. M. Efficient generation of permutationally invariant potential energy surfaces for large molecules. *J. Chem. Theory Comput.* **16**, 3264–3272 (2020).
28. MSA software with gradients. <https://github.com/szquchen/MSA-2.0> (2019). Accessed: 2019-01-20.
29. Anderson, J. B. A random-walk simulation of the Schrödinger equation:  $\text{H}_3^+$ . *J. Chem. Phys.* **63**, 1499–1503 (1975).
30. Kosztin, I., Faber, B. & Schulten, K. Introduction to the diffusion Monte Carlo method. *Am. J. Phys.* **64**, 633–644 (1996).
31. Anderson, J. B. Quantum chemistry by random walk.  $\text{H}^2\text{P}$ ,  $\text{H}_3^+ D_{3h}^1 A'_1$ ,  $\text{H}_2^3\Sigma_u^+$ ,  $\text{H}_4^1\Sigma_g^+$ ,  $\text{Be}^1\text{S}$ . *J. Chem. Phys.* **65**, 4121–4127 (1976).
32. Wang, Y. & Bowman, J. M. One-dimensional tunneling calculations in the imaginary-frequency, rectilinear saddle-point normal mode. *J. Chem. Phys.* **129**, 121103 (2008).
33. Colbert, D. T. & Miller, W. H. A novel discrete variable representation for quantum mechanical reactive scattering via the  $S$ -matrix Kohn method. *J. Chem. Phys.* **96**, 1982–1991 (1992).

## Acknowledgment

JMB thanks the ARO, DURIP grant (W911NF-14-1-0471), for funding a computer cluster where most of the calculations were performed and current financial support from NASA (80NSSC20K0360). We are thankful for correspondence with Markus Meuwly and Silvan Käser.

## **Author Contributions**

CQ and PLH performed the calculations. CQ, PLH, RC, and AN developed the computational software needed for the fitting basis sets and  $\Delta$ -machine learning approach. JMB designed and led the research. All authors contributed to write the manuscript.

## **Competing financial interests**

The authors declare no competing financial interests.

## **Data Availability**

Data supporting the findings of this study are available from the corresponding authors upon reasonable request.

## **Code Availability**

The code employed to generate the fitting basis sets will be made publicly available.